

# Core-Periphery Structure in Networks

M. Puck Rombach

Oxford Centre for Industrial and Applied Mathematics  
 University of Oxford  
 rombach@maths.ox.ac.uk

Mason A. Porter

Oxford Centre for Industrial and Applied Mathematics  
 Complex Agent-Based Dynamic Networks  
 University of Oxford  
 porterm@maths.ox.ac.uk

James H. Fowler

Department of Political Science  
 School of Medicine  
 University of California  
 jhfowler@ucsd.edu

Peter J. Mucha

Department of Mathematics  
 Carolina Center for Interdisciplinary Applied Mathematics  
 University of North Carolina  
 mucha@unc.edu

November 23, 2018

## Abstract

Intermediate-scale (or ‘meso-scale’) structures in networks have received considerable attention, as the algorithmic detection of such structures makes it possible to discover network features that are not apparent either at the local scale of nodes and edges or at the global scale of summary statistics. Numerous types of meso-scale structures can occur in networks, but investigations of meso-scale network features have focused predominantly on the identification and study of community structure. In this paper, we develop a new method to investigate the meso-scale feature known as *core-periphery structure*, which consists of an identification of a network’s nodes into a densely connected core and a sparsely connected periphery. In contrast to traditional network communities, the nodes in a core are also reasonably well-connected to those in the periphery. Our new method of computing core-periphery structure can identify multiple cores in a network and takes different possible cores into account, thereby enabling a detailed description of core-periphery structure. We illustrate the differences between our method and existing methods for identifying which nodes belong to a core, and we use it to classify the most important nodes using examples of friendship, collaboration, transportation, and voting networks.

Submitted for publication.

## 1 Introduction

Networks are used to model systems in which entities, represented by nodes, interact with each other. When representing a network as a graph, all of the connections are pairwise and hence

represented by ties known as edges [1, 2]. Such a representation has led to numerous insights in the social, natural, and information sciences, and the study of networks has in turn borrowed ideas from all of these areas [3].

Networks can be described using a mixture of local, global, and intermediate-scale (meso-scale) perspectives. Accordingly, one of the key uses of network theory is the identification of summary statistics for large networks in order to develop a framework to analyze and compare complex structures [1]. In such efforts, the algorithmic identification of meso-scale network structures allows one to discover features that might not be apparent either at the local level of nodes and edges or at the global level of summary statistics.

In particular, considerable effort has gone into algorithmic identification and investigation of a particular type of meso-scale structure known as community structure [4, 5], in which cohesive groups called “communities” consist of nodes that are connected densely to each other such that the connections between nodes in different communities are comparatively sparse. Myriad methods have been developed to detect network communities [4–7], including ones that allow such groups to overlap with each other [8–10]. These efforts have met with some success, as they have led to insights in applications such as committee [11] and voting [12] networks in political science, friendship networks at universities [13] and other schools [14], protein-protein interaction networks [15], and mobile phone networks [16].

Although (and arguably because) community structure has been very successful [4, 5], the investigation of other types of meso-scale structure—often in the form of different “block models” [5]—has received much less attention than it deserves. The type of meso-scale network structure that we consider in the present paper is known as *core-periphery structure* and was first proposed by Borgatti and Everett in 1999 [17]. There have been a few attempts to advance this methodology [17–19], but they typically rely on implementations of the original method [17] in the software package UCInet [20], and there has been little other development since.

A core-periphery structure of a network is a division of the nodes into a densely connected core and a sparsely connected periphery. The nodes in the core should also be reasonably well-connected to the nodes in the periphery, but nodes in the periphery are not well-connected to the core. Hence, a node belongs to the core if and only if it is well-connected both to other nodes in the core and to nodes assigned to the periphery. A core structure in a network is thus not merely densely connected but also tends to be “central” to the network in terms of short paths through the network. The latter feature also helps to distinguish core-periphery structure from community structure. Importantly, networks can have nested core-periphery structure as well as both core-periphery structure and community structure, so it is desirable to develop algorithms that allow one to simultaneously examine both types of meso-scale structures.

Several results underscore the importance of considering core-periphery structure in addition to community structure. For example, Fan Chung and Linyuan Lu [21] showed that power-law random graphs, in which the number of nodes of degree  $k$  is proportional to  $k^{-\beta}$ , almost surely contain a dense subgraph that has short distance to almost all other nodes in the graph when the exponent  $\beta \in (2, 3)$ . This suggests that it is sensible for networks with heavy-tailed degree distributions to contain some sort of cohesive core, and there is strong evidence that this is indeed the case in many real-world networks (such as many social networks and the World Wide Web) [1, 2, 22].

Additionally, nodes of particularly high degree, called ‘hubs’, occur in many real-world networks and can pose a problem for community detection, as they often are connected to nodes in many parts of a network and can thus have strong ties to several different communities. For instance, such

nodes might be assigned to different communities by the use of different computational heuristics applied to the same notion of community [23], and it becomes crucial to consider their strengths of membership across different communities (e.g., by using a method that allows overlapping communities) [9, 10]. This suggests, moreover, that in such situations the usual notion of a community might not be ideal for achieving an optimal understanding of the meso-scale network structure that is actually present and that considering hubs to be part of a core in a core-periphery structure might be more appropriate [24].

The rest of this paper is organized as follows. We first describe previously proposed methods for detecting core-periphery structure in networks before presenting our new method, called *Core Score*, which computes a continuous value along a core-periphery spectrum and thereby yields a centrality measure based on core-periphery structures in the network. We illustrate our method using a set of synthetic (computer-generated) benchmark random networks with a known core. We then apply our method to several real-world networks: the Zachary Karate Club, collaboration networks of network scientists, and United States Congressional voting networks. We conclude by summarizing our results and include additional results—including an application to the London Underground (‘The Tube’) transportation network—in an online Supplementary Information.

## 2 Detecting Core-Periphery Structure

### 2.1 Existing Methods

Intuitively, one expects many real-world networks to possess some sort of core-periphery structure as part of their meso-scale structure. Methods proposed to measure the core-periphery structure of a network include block models [17],  $k$ -core organization [18], and aggregation of information about connectivity and short paths through the network [19].

The notion of a core-periphery structure was formalized in social networks by Borgatti and Everett in 1999 [17], who proposed algorithms for detecting both discrete and continuous versions of core-periphery structure in weighted, undirected graphs. Their discrete notion of core-periphery structure is based on comparing a network to an ideal block model that consists of a fully-connected core and a periphery that has no internal edges but is fully connected to the core. Their algorithm aims to find a vector  $C$  of length  $n$  whose entries can either be 1 or 0. The  $i$ th entry  $C_i$  equals 1 if the corresponding node is assigned to the core, and it is 0 if the corresponding node is assigned to the periphery. Let  $C_{ij} = 1$  if  $C_i = 1$  or  $C_j = 1$  and  $C_{ij} = 0$  otherwise, and define

$$\rho_C = \sum_{i,j} A_{ij} C_{ij}, \quad (1)$$

where  $A_{ij}$  are the elements of the graph’s adjacency matrix. The matrix element  $A_{ij}$  represents the strength (i.e., weight) of the tie between nodes  $i$  and  $j$ , and it equals 0 if nodes  $i$  and  $j$  are not connected. The Borgatti-Everett algorithm seeks a value of  $\rho_C$  that is high compared to the expected value of  $\rho$  if  $C$  is shuffled such that the number of 1 and 0 entries are preserved but their order is randomized. The output is the vector  $C$  that gives the highest  $z$ -score for  $\rho_C$ .

As a variation of the above discrete notion of core-periphery structure, Borgatti and Everett defined

$$C_{ij} = \begin{cases} 1, & \text{if } C_i \text{ and } C_j = 1, \\ a \in [0, 1], & \text{if } C_i = 1 \text{ or } C_j = 1, \\ 0, & \text{otherwise.} \end{cases} \quad (2)$$

They also defined a continuous notion of core-periphery structure in which a node is assigned a ‘coreness’ value of  $C_i$  and  $C_{ij} = C_i \times C_j = a$ . Our method to study core-periphery structure in weighted, undirected networks is motivated by the continuous formulation of Borgatti and Everett. Before discussing our approach, we call attention to two other methods in the literature.

In 2005, Holme defined a core-periphery coefficient [18]

$$c_{cp}(G) = \frac{C_C(V_{core}(G))}{C_C(V(G))} - \left\langle \frac{C_C(V_{core}(G'))}{C_C(V(G'))} \right\rangle_{G' \in \mathcal{G}(G)}, \quad (3)$$

where the angled brackets indicate the average and  $\mathcal{G}(G)$  is an ensemble of graphs with the same degree sequence as the unweighted, undirected graph  $G$  and

$$C_C(U) = \left( \left\langle \langle P(i, j) \rangle_{j \in V \setminus \{i\}} \right\rangle_{i \in U} \right)^{-1}, \quad (4)$$

and  $P(i, j)$  is the distance (i.e., number of edges in the shortest path) between nodes  $i$  and  $j$ . A  $k$ -core of the graph  $G$  is a maximal connected subgraph in which all nodes have degree at least  $k$ , and  $V_{core}$  is the  $k$ -core with maximal  $C_C(U)$ . Using  $k$ -cores to examine core-periphery structure is computationally fast (and we note that one could, in principle, generalize Holme’s method for weighted graphs), but it entails very strong restrictions on the notion of a network core.

One expects the core of a network to have high connectivity to other parts of the network, so Da Silva *et al.* introduced a measure of connectivity known as network *capacity* [19]:

$$K = \sum_{l=1}^M P_l^{-1}, \quad (5)$$

where  $M$  is the total number of connected pairs of nodes and  $P_l$  is the length of the shortest path between the  $l$ th pair of nodes. Da Silva *et al.* then defined a core coefficient as  $cc = N'/N$ , where  $N$  is the total number of nodes in the network,  $N'$  satisfies  $\sum_{m=0}^{N'} K_m = 0.9 \sum_{u=0}^N K_u$ , and  $K_m$  is the capacity of the network after the removal of  $m$  nodes. The nodes are removed in order of closeness centrality, which is defined as the mean shortest path from a node to each of the other nodes in a network [19]. Note that in the remainder of this paper, we will use the following definition for closeness centrality of a node  $j$  (there are several different ones available in the literature):

$$CC_j = \frac{1}{N} \sum_{i \in V} P(i, j),$$

where  $P(i, j)$  is the sum of edge weights in a shortest path in the context of weighted networks. Da Silva *et al.* considered only binary networks, but their method can be generalized straightforwardly to weighted networks.

## 2.2 Our Method

Our method to study core-periphery structure in weighted, undirected networks is motivated by the continuous formulation of Borgatti and Everett described above.

We allow the vector  $C$  to take non-negative values, and we let  $C_{ij} = C_i \times C_j$ . We seek a core vector  $C$  that is normalized (so that the entries sum to 1) and is a shuffle of the vector  $C^*$  whose components specify the *local core values*

$$C_m^* = \frac{1}{1 + \exp \{-(m - N\beta) \times \tan(\pi\alpha/2)\}}, \quad (6)$$

such that the *core quality*

$$R = \sum_{i,j} A_{ij} C_i C_j \quad (7)$$

is maximized. There are two parameters:  $\alpha \in [0, 1]$  and  $\beta \in [0, 1]$ . The parameter  $\alpha$  sets the sharpness of the boundary between the core and the periphery. The value  $\alpha = 0$  yields the fuzziest boundary and  $\alpha = 1$  gives the sharpest transition (i.e., a binary transition): as  $\alpha$  varies from 0 to 1, the maximum slope of  $C^*$  varies from 0 to  $\infty$ . The parameter  $\beta$  sets the size of the core: as  $\beta$  varies from 0 to 1, the number of nodes included in the core varies from  $N$  to 0. We define the total *core score* of each node  $i$  as

$$CS(i) = Z \sum_{\alpha,\beta} \left( C_i^*(\alpha, \beta) \times \sum_{j \in \Gamma(i)} C_j^*(\alpha, \beta) \right), \quad (8)$$

where  $\Gamma(i)$  is the set of neighbours of node  $i$  and the normalization factor  $Z$  is chosen so that  $\max_k [CS(k)] = 1$ . We note, additionally, that core score gives a new notion of network centrality [1, 22]

In the results presented in this paper, we assign the values of  $C_i^*(\alpha, \beta)$  to maximize  $R$  using a simulated-annealing algorithm [25] (see the online Supplementary Information for details of the procedure). Other algorithms may be faster, especially those in which the choices for  $\alpha$  and  $\beta$  depend on the structure of the network. The purpose of this paper, however, is to introduce a novel notion of core-periphery structure, so we leave the question of which algorithm is most efficient to future work.

### 3 Synthetic Benchmark Networks

We test our method on an ensemble of random networks with an artificial core-periphery structure. In designing these synthetic networks, we are motivated by the fact that networks can have both community structure and core-periphery structure. In Fig. 1, we show images of the adjacency matrices of different idealized block models, which illustrate (a) community structure, (b) core-periphery structure, (c) a global core-periphery structure with a local community structure, and (d) a global community structure with a local core-periphery structure. By permuting rows and columns of the adjacency matrix, one can see that (c) and (d) are, in fact, equivalent.

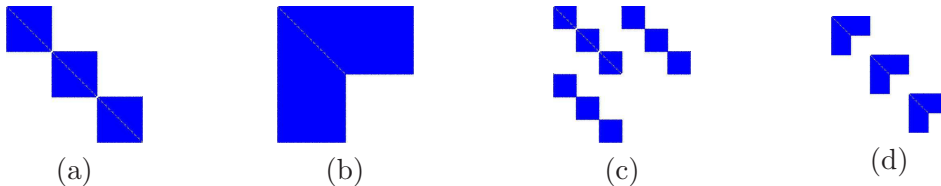


Figure 1: Different network block models. (a) Community structure, (b) core-periphery structure, (c) global core-periphery structure with local community structure, and (d) global community structure with local core-periphery structure. Note that (c) and (d) are equivalent.

### 3.1 Artificial Core-Periphery Structure

We develop a family of synthetic networks that only have a core-periphery structure [see Fig. 1(b)], and we call these networks  $CP(N, d, p, k)$ . (We will consider networks with both core-periphery structure and community structure when we examine real-world networks.) Each network in the ensemble  $CP(N, d, p, k)$  has  $N$  nodes, where  $dN$  of the nodes are core nodes,  $(1 - d)N$  of the nodes are periphery nodes, and  $d \in [0, 1]$ . The edges are assigned independently at random. The edge probabilities for periphery-periphery, core-periphery, and core-core pairs are  $p$ ,  $kp$ , and  $k^2p$ , respectively. Note that  $p \in [0, 1]$  and  $k \in [1, (1/p)^{1/2}]$ . We fix  $N = 100$ ,  $d = \frac{1}{2}$ , and  $p = \frac{1}{4}$  and compute the core-periphery structure for 100 different instances of this random graph ensemble for each of the parameter values  $k = 1, 1.1, 1.2, \dots, 2$ . We show our results in Fig. 2. These synthetic networks have a discrete core-periphery structure, whereas our algorithm outputs a continuous ranking, which we recall makes core score a notion of centrality.

In Fig. 2, we display the fraction of nodes that are correctly identified as one of the top 50 core nodes (because the networks have  $Nd = 50$  core nodes by construction). We compare our results to those obtained using the continuous core-detection algorithm in UCINet using the so-called “minres” algorithm in Version 6.289 [20]. (Whenever two nodes had an identical score, the tie was broken at random.) We also show the results of attempting to determine the core nodes using various types of centrality, which are designed to measure notions of importance of nodes.

In Core Score, which examines core-periphery structure as a new kind of centrality, nodes are more likely to be part of a network’s core both if they have high strength and if they are connected to other nodes in the core. The latter idea is reminiscent of ideas like eigenvector centrality and PageRank centrality, which recursively define nodes as important based on having connections to other nodes that are important [1]. We will also compare Core Score with various notions of centrality below when we discuss our example of political voting networks.

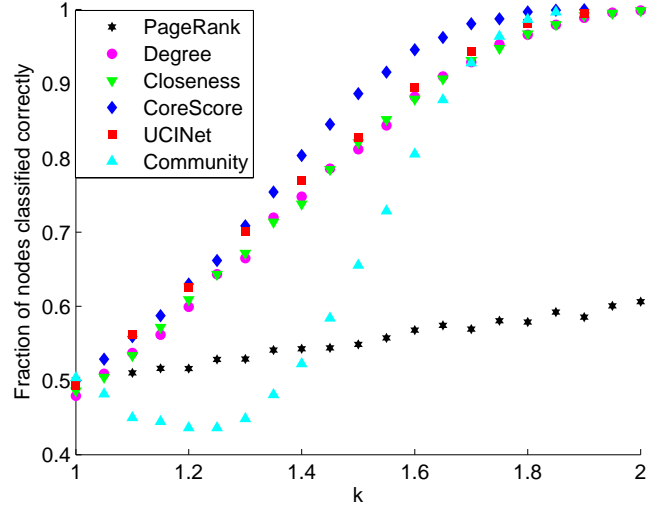


Figure 2: Fraction of core nodes correctly identified by computing core score for random networks  $CP(100, .5, .25, k)$  averaged over 100 realizations. We compare this fraction to those obtained using the continuous core-detection algorithm in UCINet (Version 6.289) and various other types of centralities.

## 4 Real Networks

In this section, we examine core-periphery structures in several real-world data sets. We consider another example in the online Supplementary Information.

### 4.1 The Zachary Karate Club

We first consider the infamous Zachary Karate Club [26], which consists of friendship ties between 34 members of a university karate club in the U.S. in the 1970s (we used the unweighted version for this purpose). A conflict led the club to split into two new clubs, and this network has become one of the standard benchmark examples for investigations of community structure [4,5]. We visualize the network in Fig. 3, where we have identified the nodes according to the split that occurred as a result of a longstanding disagreement between the instructor, Mr. Hi, and the club president, John A.<sup>1</sup>. These two primary actors are represented by nodes 1 and 34, respectively.

Table 1 shows the nodes with their global core values, which we computed using Core Score. Unsurprisingly, the main actors (nodes 1 and 34) have the highest mean core scores. One can see more structure by considering all values of the parameters  $\alpha$  and  $\beta$  rather than averaging over them. In particular, the fact that node 1 has the highest mean core value does not imply that it has the highest value of  $C_1^*(\alpha, \beta)$  for all  $\alpha$  and  $\beta$ . In Fig. 4, we show how the top node varies with respect to  $\alpha$  and  $\beta$ . Node 1 has the highest core value only 16% of the time, whereas node 34 is the top node 44% of the time.

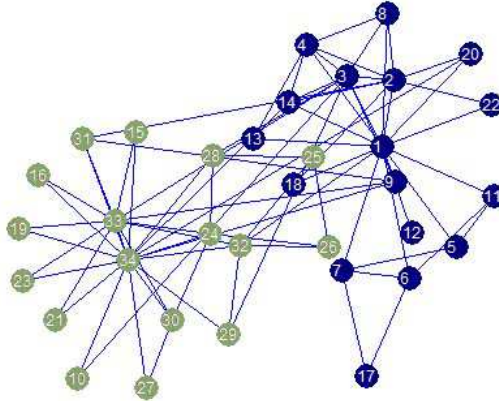


Figure 3: The Zachary Karate Club network [26], visualized using the implementation of the Kamada-Kawai algorithm [27] of Ref. [28]. The colors represent the two groups into which the club split while it was under study.

One can illustrate this result by plotting the core quality  $R$  (7) as a function of  $\alpha$  and  $\beta$  (see Fig. 5). The regions in which node 1 has the highest Core Score typically correspond to those in

---

<sup>1</sup>These names are pseudonyms introduced in Ref. [26]

Table 1: Nodes in the Zachary Karate Club network nodes along with their global core values.

Node	Core Score	Node	Core Score
1	1.0000	6	.0681
34	.8876	26	.0641
3	.8487	25	.0631
2	.7720	11	.0455
33	.7126	5	.0448
4	.5927	22	.0347
14	.4740	18	.0345
9	.4658	15	.0296
8	.3827	21	.0296
31	.3192	23	.0287
24	.2763	16	.0284
32	.2507	19	.0278
30	.2149	10	.0275
20	.1569	13	.0265
28	.1248	27	.0162
29	.1128	17	.0135
7	.0702	12	.0027

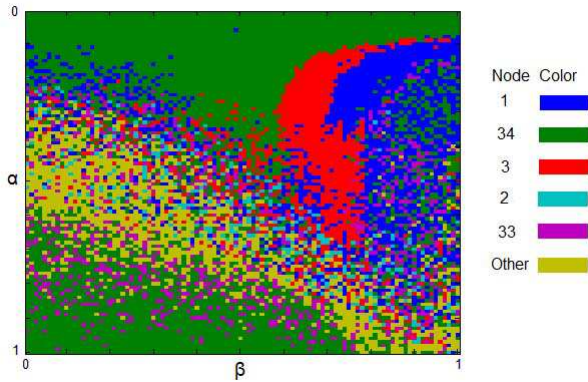


Figure 4: The Zachary Karate Club network’s top Core Score node as a function of  $\alpha$  and  $\beta$ .

which the aggregate core score (i.e., the core quality  $R$ ) is the highest in Fig. 5. One can distinguish one band for each of the top three nodes (node 34 in green, node 3 in red, and node 1 in blue). The areas in which node 1 has the top Core Score are those in which the core size is smallest. Although node 34 has a slightly higher degree, node 1 has the densest small core of blue nodes around it. As the core size becomes larger, more of the red nodes are added to the core and node 3, which has more connections to red nodes, becomes more important to the network than node 1. As the core becomes very large, node 34 ends up at the top simply because it has the highest degree. The landscape of top core nodes can be very complicated, especially as one considers larger networks, but it provides a good illustration of how Core Score works in the case of the Zachary Karate Club.

## 4.2 The London Underground

We compute core values for the London Underground (‘Tube’) transportation network, which exhibits a strong core-periphery structure but a weak community structure. We collected the data

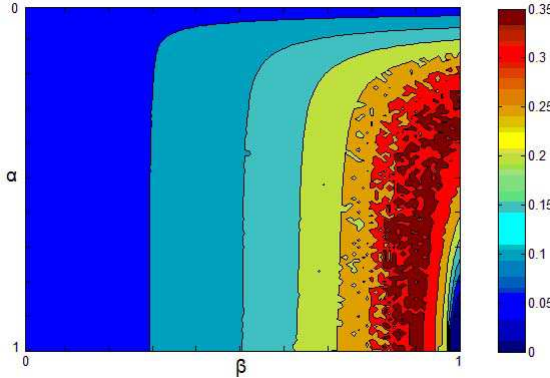


Figure 5: The Zachary Karate Club core quality ( $R$ ) score as a function of the parameters  $\alpha$  and  $\beta$ .

for this example using the website for the London Underground (<http://www.tfl.gov.uk>). The Tube network that we assembled has 317 nodes (one for each station) and weighted edges that represent the number of direct, contiguous connections between two stations. For example, Baker Street and Paddington share an edge of weight 2, as they are adjacent stations on the Circle Line and the Hammersmith & City Line. They are also connected by the Bakerloo Line; however, they are not adjacent stations on this line, so it does not affect the weight of the edge between them.

Community detection (as detected by optimizing modularity at the default resolution value using the Louvain [29] algorithm) splits this network into 21 communities, with the largest community of size 19. Most of these communities are formed by groups of stations on a single line. Hence, these communities do not appear to give much information about this network.

Table 2 shows the result of applying the Core Score method to the London Tube network. We list the top ten stations and their corresponding Core Scores.

Node	Core Score
King's Cross St. Pancras	1.0000
Baker Street	0.8339
Waterloo	0.8175
Willesden Junction	0.7973
Bank	0.7789
West Ham	0.7516
Green Park	0.7447
Oxford Circus	0.7200
Liverpool Street	0.7167
Paddington	0.6799

Table 2: The ten most core-like nodes in the London Underground network along with their Core Scores.

### 4.3 Networks of Network Scientists

We now consider networks of co-authorships between scientists working on network science. We study two such networks—one from 2006 [30] and another from 2010 [31]. These networks, which both concentrate on papers written by physicists, have 379 and 552 nodes, respectively, in their largest connected components. The nodes correspond to scholars working in the field of network science, and an edge between two of them has a weight based on the number of papers that they have co-authored. (Note that the 2006 network is not a subset of the 2010 network.) We show the names of the scientists with the top thirty core scores for both networks in Table 2 in the Supplementary Information.

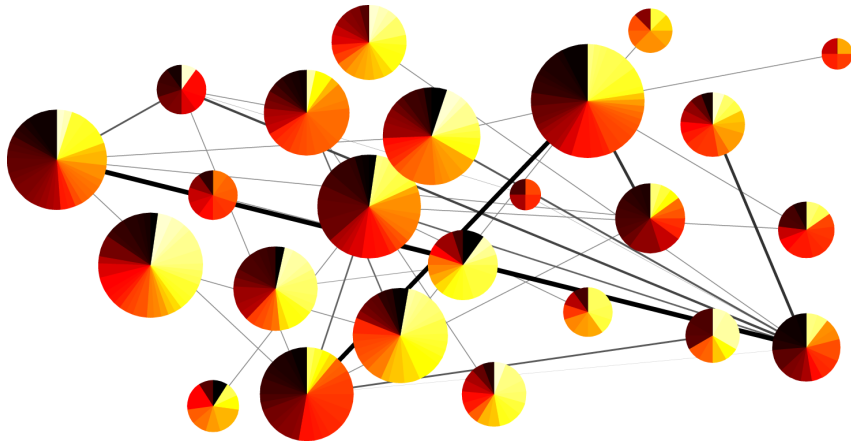


Figure 6: Visualization of the 2010 network of network scientists. Each pie chart represents a community and the colors represent the Core Score rank order of its members. Each pie segment represents a single node, and larger pies contain more nodes. We located the centers of the communities using the Kamada-Kawai algorithm [27, 28], using the code described in Ref. [28].

The networks of network scientists give a pair of examples that have both sensible community structure and sensible core-periphery structure [recall the block model in Fig. 1(c) and (d)]. We illustrate this point in our visualization of the network in Fig. 6. Each pie chart represents a community, as detected by optimizing modularity using the Louvain [29] algorithm. Each pie is composed of the nodes in a single community, and each node is colored according to its Core Score. One can plainly see that the network’s core is distributed throughout the various communities, and that each community has both core and periphery nodes.

The selected community detection implementation splits the 2006 network into 19 communities and the 2010 network into 25 communities, although different community detection heuristics and random seeds will yield somewhat different sets of groups [23]. For example, one previous examination [32] of the community structure of the 2006 network of network scientists identified and described a variety of partitions, (the highest modularity there coming by way of a divisive spectral routine which initially separates the connected component into three large groups: one in which A.-L. Barabási is the key node (in the sense of having the largest community centrality in the group), one in which M. E. J. Newman is the key node, and one in which A. Vespignani and R. Pastor-Satorras are the two key nodes. As shown in Table 2 in the Supplementary Information, all four of these nodes have very high Core Scores.

The communities in both the 2006 and 2010 networks exhibit a core-periphery structure. Each of the communities in the two networks of network scientists are composed of one or two highly connected nodes and several other nodes with low strengths. In the 2006 network, the mean strength is 4.8, and 17 of the 19 communities contain a node with strength at least 9. (There are 43 such nodes in the entire network.) In the 2010 network, the mean strength is 4.7, and 20 of the 25 communities contain a node of at least strength 10. (There are 50 such nodes in the entire network.) Additionally, as indicated above, the core nodes are distributed throughout the communities. In the 2006 network, 12 of the 19 communities contain at least one node among those with the top 30 Core Scores; in the 2010 network, 9 of the 25 communities contain at least one node in the top 30.

#### 4.4 U.S. Congress Voting Network

Finally, we consider United States Congress roll-call similarity networks. One can build such a network from a single 2-year Congress of either the Senate or the House of Representatives [33–35]. For each House and Senate, one constructs a complete weighted network in which a node represents a legislator and the edge between two legislators gives the fraction of bills on which they both voted in the same manner. That is, the adjacency matrix element  $A_{ij}$  is equal to the number of times that legislator  $i$  and  $j$  voted in the same way divided by the total number of bills on which both  $i$  and  $j$  cast a vote. This type of network is called a “similarity network”, because the weights of the edges represent a measure of similarity between the nodes to which they are incident.

We look at the similarity network of the 108<sup>th</sup> Senate, which occurred during the third and fourth year of George W. Bush’s presidency (2003–2005). We give the individual Core Score for each Senator in Table 3 of the Supplementary Information. In Fig. 7, we show scatter plots between the strength centrality and different other centrality measures for the 108<sup>th</sup> Senate network. We color Republicans in red and Democrats in blue. Notice how community centrality shows a negative correlation with strength centrality [30]. Figure 2 confirms that this is sensible: in our synthetic networks, community centrality gives a higher rating to periphery nodes than to core nodes when the two types of nodes have similar densities.

Some of the centrality measures in Fig. 7 have been used previously to study Senators and Representatives in legislation cosponsorship networks [37, 38], which have in turn been compared to modularity-based measures of political partisanship studied using roll-call voting networks [39]. As one can see from Fig. 7, these different centrality measures do indeed measure different things. Observe that, in this example, none of the centrality measures by themselves separate the communities very well, whereas a combination of two of them often does. Investigation of core-periphery structure using Core Scores thus complements examination of community structure by allowing one to examine a different type of meso-scale structure in networks such as Congressional voting networks. It also nicely complements existing centrality measures.

### 5 Conclusions and Discussion

In conclusion, we have proposed a new method to investigate core-periphery structure in networks. This complements investigations of network community structure, which has been considered at great length and from myriad perspectives. By contrast, there are comparatively few methods to study core-periphery structure, which we believe is just as important as community structure. As we have illustrated, networks can contain community structure, core-periphery structure, or both.

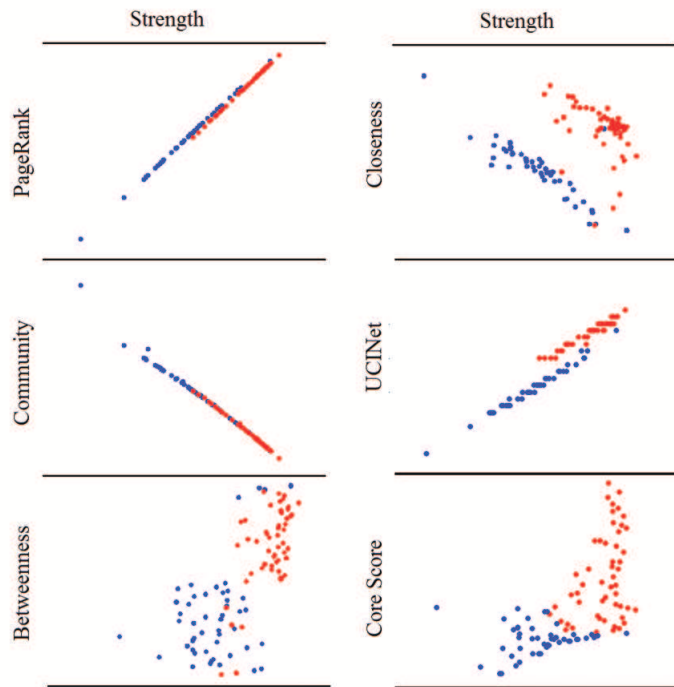


Figure 7: Scatter plots between strength and various centrality measures for the 108<sup>th</sup> Senate network. The betweenness centrality was obtained by turning the network into a binary network (threshold: .6) and using code from [36].

For example, the 2006 and 2010 networks of network scientists clearly exhibit both types of meso-scale structures. In these networks the core-periphery structure reveals a global ‘infrastructure’ that remains invisible if one searches only for community structure.

In contrast to the wealth of attention given to community structure over the last decade, the development of new methods to examine core-periphery structure is in its infancy. We have shown using a synthetic family of networks that our method performs well in detecting artificial core-periphery structures. The purpose of the present paper is conceptual development, and our current implementation of our method is very slow because of its use of simulated annealing. Moreover, we considered 10000 different values of  $(\alpha, \beta)$  in each use of the method, but this should not be necessary, so one can also speed up the method by intelligent choice of which parameter values to consider.

Many networks contain meso-scale structures in addition to (or instead of) community structure, and continued pursuit of methods to investigate them should prove fruitful. As we have illustrated, core-periphery structure provides one example that is worth further attention.

## 5.1 Acknowledgements

We thank Charlie Brummit, Sergey Dorogovtsev, José Mendes, and Jim Moody for useful conversations. This work was funded by the James S. McDonnell Foundation (# 220020177) and the NSF (DMS-0645369) and was carried out in part at the Statistical and Applied Mathematical Sciences Institute in Research Triangle Park, North Carolina. We thank Mark Newman for providing the data for the Zachary Karate Club network and the 2006 network of network scientists, Martin Rosvall for providing the data for the 2010 network of network scientists, and Keith Poole and Howard Rosenthal for maintaining the Congressional voting data at [www.voteview.com](http://www.voteview.com) [33]. The simulated annealing MATLAB code that we used was written by Joachim Vandekerckhove [40].

## References

- [1] Newman, M. E. J. (2010) *Networks: An Introduction*. (OUP Oxford).
- [2] Boccaletti, S, Latora, V, Moreno, Y, Chavez, M, & Hwang, D.-U. (2006) *Physics Reports* **424**, 175–308.
- [3] Barabási, A.-L. (2005) *Nature Physics* **1**, 68–70.
- [4] Porter, M. A, Onnela, J.-P, & Mucha, P. J. (2009) *Notices of the American Mathematical Society* **56**, 1082–1097, 1164–1166.
- [5] Fortunato, S. (2010) *Physics Reports* **486**, 75–174.
- [6] Girvan, M & Newman, M. E. J. (2002) *Proceedings of the National Academy of Sciences* **99**, 7821–7826.
- [7] Newman, M. E. J & Girvan, M. (2004) *Physical Review E* **69**, 026113.
- [8] Palla, G, Derenyi, I, Farkas, I, & Vicsek, T. (2005) *Nature* **435**, 814–818.
- [9] Ahn, Y.-Y, Bagrow, J. P, & Lehmann, S. (2010) *Nature* **466**, 761–764.

[10] Ball, B, Karrer, B, & Newman, M. E. J. (2011) *Physical Review E* **84**, 036103.

[11] Porter, M. A, Mucha, P. J, Newman, M. E. J, & Warmbrand, C. M. (2005) *Proceedings of the National Academy of Sciences* **102**, 7057–7062.

[12] Mucha, P. J, Richardson, T, Macon, K, & Onnela, M. A. P. J.-P. (2010) *Science* **328**, 876–878.

[13] Traud, A. L, Kelsic, E. D, Mucha, P. J, & Porter, M. A. (2011) *SIAM Review* **53**, 526–543.

[14] González, M. C, Herrmann, H. J, Kertesz, J, & Vicsek, T. (2007) *Physica A* **379**, 307–316.

[15] Lewis, A. C. F, Jones, N. S, Porter, M. A, & Deane, C. M. (2010) *BMC Systems Biology* **4**.

[16] Onnela, J.-P, Saramäki, J, Hyvönen, J, Szabó, G, Lazer, D, Kaski, K, Kertész, J, & Barabási, A.-L. (2007) *Proceedings of the National Academy of Sciences* **104**, 7332–7336.

[17] Borgatti, S. P & Everett, M. G. (1999) *Social Networks* **21**, 375–395.

[18] Holme, P. (2005) *Physical Review E* **72**, 046111.

[19] da Silva, M. R, Ma, H, & Zeng, A.-P. (2008) *Proceedings of the IEEE* **96**, 1411–1420.

[20] Borgatti, S. P, Everett, M. G, & Freeman, L. C. (2011) Ucinet. Version 6.289, available at <http://www.analytictech.com/ucinet/>.

[21] Chung, F & Lu, L. (2002) *Proc. of the National Academy of Sciences* **99**, 15879–15882.

[22] Wasserman, S & Faust, K. (1994) *Social Network Analysis: Methods and Applications*, Structural Analysis in the Social Sciences. (Cambridge University Press, Cambridge, UK).

[23] Good, B. H, de Montjoye, Y.-A, & Clauset, A. (2010) *Physical Review E* **81**, 046106.

[24] Leskovec, J, Lang, K. J, Dasgupta, A, & Mahoney, M. W. (2009) *Internet Mathematics* **6**, 29–123.

[25] Kirkpatrick, S, Gelatt, Jr., C. D, & Vecchi, M. P. (1983) *Science* **220**, 671–680.

[26] Zachary, W. W. (1977) *Journal of Anthropological Research* **33**, 452–473.

[27] Kamada, T & Kawai, S. (1988) *Information Processing Letters* **31**, 7–15.

[28] Traud, A, Frost, C, Mucha, P. J, & Porter, M. A. (2009) *Chaos* **19**.

[29] Blondel, V. D, Guillaume, J.-L, Lambiotte, R, , & Lefebvre, E. (2008) *Journal of Statistical Mechanics: Theory and Experiment*.

[30] Newman, M. E. J. (2006) *Physical Review E* **74**, 036104.

[31] Edler, D & Rosvall, M. (2010) The map generator software package.

[32] Richardson, T, Mucha, P. J, & Porter, M. A. (2009) *Physical Review E* **80**, 036111.

[33] Poole, K. T. (2011) Voteview. <http://voteview.com>.

- [34] Poole, K. T & Rosenthal, H. (1997) *Congress: A Political-Economic History of Roll Call Voting*. (Oxford University Press, Oxford, United Kingdom).
- [35] Waugh, A. S, Pei, L, Fowler, J. H, Mucha, P. J, & Porter, M. A. (2010) *arXiv:0907.3509*.
- [36] Gleich, D. F. (2009) Ph.D. thesis (Stanford University). Chapter 7 on MatlabBGL.
- [37] Fowler, J. H. (2006) *Political Analysis* **14**, 454–465.
- [38] Fowler, J. H. (2006) *Social Networks* **28**, 456–487.
- [39] Zhang, Y, Friend, A. J, Traud, A. L, Porter, M. A, Fowler, J. H, & Mucha, P. J. (2008) *Physica A* **387**, 1705–1712.
- [40] Vandekerckhove, J. (2008) General simulated annealing algorithm (<http://www.mathworks.de/matlabcentral/fileexchange/10548>).

## Supplementary Information

### Simulated Annealing

The simulated annealing Matlab code we used for the purpose of this paper was written by Joachim Vandekerckhove [40], using the following parameters. Initial temperature: 1, stop temperature:  $10^{-8}$ , cooling schedule:  $.8*T$ , maximum number of consecutive rejections: 1000, maximum number of tries within one temperature: 300, maximum number of successes within one temperature: 20.

### Network of Network Scientists

Table 3 show the names and Core Scores of the top 30 nodes for both the 2006 and 2010 network of network scientists.

NNS2006 Node	Core Score	NNS2010 Node	Core Score
Barabási, A.-L.	1.00	Barabási, A.-L.	1.00
Jeong, H.	0.92	Jeong, H.	0.88
Oltvai, Z. N.	0.69	Boccaletti, S.	0.67
Newman, M. E. J.	0.60	Newman, M. E. J.	0.65
Pastor-Satorras, R.	0.56	Latora, V.	0.62
Moreno, Y.	0.43	Vicsek, T.	0.51
Vespignani, A.	0.43	Pastor-Satorras, R.	0.49
Vicsek, T.	0.40	Kahng, B	0.49
Boccaletti, S.	0.40	Oltvai, Z. N.	0.49
Vazquez, A.	0.36	Moreno, Y	0.48
Holme, P.	0.34	Arenas, A.	0.46
Kahng, B.	0.33	Vespignani, A.	0.43
Diaz-Guilera, A.	0.33	Diaz-Guilera, A.	0.39
Guimerà, R.	0.32	Kurths, J.	0.37
Sole, R.	0.32	Kertesz, J.	0.37
Amaral, L. A. N.	0.31	Guimerà, R.	0.37
Kurths, J.	0.31	Caldarelli, G.	0.36
Ravasz, E.	0.31	Amaral, L. A. N.	0.35
Barthelemy, M.	0.29	Crucitti, P.	0.33
Albert, R.	0.29	Vazquez, A.	0.32
Arenas, A.	0.28	Barthelemy, M.	0.32
Neda, Z.	0.28	Solé, R. V.	0.30
Kim, B.	0.25	Kleinberg, J.	0.30
Farkas, I.	0.24	Fortunato, S.	0.30
Latora, V.	0.24	Porter, M. A.	0.28
Schubert, A.	0.23	Farkas, I. J.	0.27
Boguna, M.	0.23	Ravasz, E.	0.27
Watts, D. J.	0.21	Tomkins, A. S.	0.27
Caldarelli, G.	0.21	Goh, K. I.	0.26
Strogatz, S. H.	0.19	Kaski, K.	0.26

Table 3: The 30 nodes with the top Core Scores from the 2006 (left) and 2010 (right) networks of network scientists.

### Core Score and UCINet correlation plot for the 108<sup>th</sup> Senate

In Figure 8 we have plotted the correlation scatter plot between the continuous core scores of the 108<sup>th</sup> Senate for Core Score and the MINRES algorithm in UCINet respectively. The individual Core Score of each Senator can be found in Table 4. Republicans were the majority party in the 108<sup>th</sup> Senate, so they tend to have higher Core Scores than Democrats. A notable exception is Zell Miller [D - GA], whose collaboration and common voting patterns with Republican Congressmen is well-known [11, 39]. The Democrat with the second highest Core Score is John Kerry [D - MA], the 2004 Democratic nominee for President.

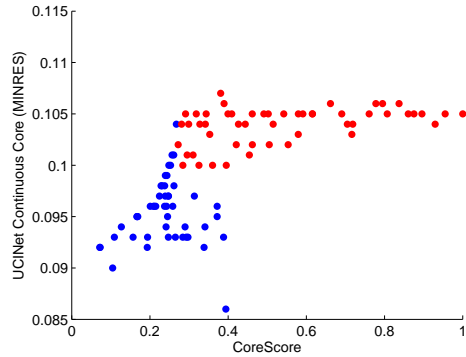


Figure 8: Correlation scatter plot between the continuous core scores of the 108<sup>th</sup> Senate, calculated with Core Score and the MINRES algorithm in UCINet respectively.

Node	Core Score	Party	Vote
■ Mitch McConnell [R - KY]	1.0000	98%	
■ Thad Cochran [R - MS]	0.9550	98%	
■ Jim Bunning [R - KY]	0.9296	97%	
■ Conrad Burns [R - MT]	0.8957	96%	
■ Bill Frist [R - TN]	0.8754	97%	
■ Orrin Hatch [R - UT]	0.8609	97%	
■ Pete Domenici [R - NM]	0.8373	96%	
■ Saxby Chambliss [R - GA]	0.8070	97%	
■ Pat Roberts [R - KS]	0.7950	97%	
■ Chuck Grassley [R - IA]	0.7779	97%	
■ Bob Bennett [R - UT]	0.7608	97%	
■ John Cornyn [R - TX]	0.7188	96%	
■ Larry Craig [R - ID]	0.7166	96%	
■ Mike Crapo [R - ID]	0.7049	96%	
■ Kit Bond [R - MO]	0.6908	96%	
■ Jim Talent [R - MO]	0.6618	97%	
■ Sam Brownback [R - KS]	0.6158	96%	
■ Ted Stevens [R - AK]	0.6156	96%	
■ Lamar Alexander [R - TN]	0.5912	97%	
■ Liddy Dole [R - NC]	0.5795	96%	
■ James Inhofe [R - OK]	0.5793	96%	
■ Craig Thomas [R - WY]	0.5535	95%	
■ George Allen [R - VA]	0.5423	96%	
■ Trent Lott [R - MS]	0.5153	95%	
■ Wayne Allard [R - CO]	0.5052	95%	
■ Richard Shelby [R - AL]	0.5028	95%	
■ Richard Lugar [R - IN]	0.4913	96%	
■ Jeff Sessions [R - AL]	0.4620	94%	
■ Chuck Hagel [R - NE]	0.4617	95%	
■ Mike Enzi [R - WY]	0.4544	94%	
■ Zell Miller [D - GA]	0.4437	38%	
■ Lindsey Graham [R - SC]	0.4263	94%	
■ Rick Santorum [R - PA]	0.4209	94%	
■ Lisa Murkowski [R - AK]	0.4092	95%	
■ John Warner [R - VA]	0.3997	94%	
■ Donald Nickles [R - OK]	0.3953	93%	
■ John Kerry [D - MA]	0.3942	98%	
■ Norm Coleman [R - MN]	0.3897	94%	
■ Paul Sarbanes [D - MD]	0.3885	96%	
■ Gordon Smith [R - OR]	0.3808	94%	
■ Debbie Stabenow [D - MI]	0.3721	96%	
■ Barbara Mikulski [D - MD]	0.3720	96%	
■ Jon Kyl [R - AZ]	0.3602	93%	
■ Peter Fitzgerald [R - IL]	0.3531	93%	
■ Ben Campbell [R - CO]	0.3439	93%	
■ Kay Bailey Hutchison [R - TX]	0.3418	92%	
■ Carl Levin [D - MI]	0.3409	95%	
■ John Edwards [D - NC]	0.3385	96%	
■ George Voinovich [R - OH]	0.3278	92%	
■ John Sununu [R - NH]	0.3255	91%	
■ Mike DeWine [R - OH]	0.3184	91%	
■ Patty Murray [D - WA]	0.3137	95%	
■ John Ensign [R - NV]	0.3103	90%	
■ Arlen Specter [R - PA]	0.2991	85%	
■ Barbara Boxer [D - CA]	0.2972	95%	
■ Judd Gregg [R - NH]	0.2953	90%	
■ Dick Durbin [D - IL]	0.2929	95%	
■ Susan Collins [R - ME]	0.2911	84%	
■ Hillary Clinton [D - NY]	0.2900	95%	
■ John McCain [R - AZ]	0.2844	84%	
■ Jack Reed [D - RI]	0.2840	95%	
■ Olympia Snowe [R - ME]	0.2810	82%	
■ Lincoln Chafee [R - RI]	0.2724	78%	
■ Ben Nelson [D - NE]	0.2676	72%	
■ Edward Kennedy [D - MA]	0.2651	94%	
■ Tim Johnson [D - SD]	0.2615	94%	
■ John Breaux [D - LA]	0.2611	74%	
■ Chuck Schumer [D - NY]	0.2584	94%	
■ Max Baucus [D - MT]	0.2566	82%	
■ Mary Landrieu [D - LA]	0.2527	85%	
■ Blanche Lincoln [D - AR]	0.2484	87%	
■ Ron Wyden [D - OR]	0.2475	93%	
■ Jon Corzine [D - NJ]	0.2473	95%	
■ Tom Daschle [D - SD]	0.2469	94%	
■ Chris Dodd [D - CT]	0.2450	94%	
■ Mark Pryor [D - AR]	0.2437	89%	
■ Maria Cantwell [D - WA]	0.2425	95%	
■ Patrick Leahy [D - VT]	0.2414	94%	
■ Evan Bayh [D - IN]	0.2396	86%	
■ Harry Reid [D - NV]	0.2394	93%	
■ Byron Dorgan [D - ND]	0.2378	91%	
■ Herb Kohl [D - WI]	0.2376	94%	
■ Kent Conrad [D - ND]	0.2310	88%	
■ Tom Carper [D - DE]	0.2285	86%	
■ Bill Nelson [D - FL]	0.2245	93%	
■ Jay Rockefeller [D - WV]	0.2150	93%	
■ Dianne Feinstein [D - CA]	0.2115	92%	
■ Jeff Bingaman [D - NM]	0.2091	92%	
■ Mark Dayton [D - MN]	0.2009	93%	
■ Daniel Akaka [D - HI]	0.1940	94%	
■ Frank Lautenberg [D - NJ]	0.1933	94%	
■ Joseph Lieberman [D - CT]	0.1688	93%	18
■ Daniel Inouye [D - HI]	0.1671	93%	
■ Joe Biden [D - DE]	0.1669	92%	
■ Tom Harkin [D - IA]	0.1570	94%	
■ James Jeffords [I - VT]	0.1269	88%	
■ Russ Feingold [D - WI]	0.1092	91%	
■ Bob Graham [D - FL]	0.1048	93%	
■ Fritz Hollings [D - SC]	0.0727	88%	
■ Robert Byrd [D - WV]	0.0717	90%	

Table 4: Scores for the 108<sup>th</sup> Congress with 18 in the Senate and 14 in the House.